

LETTER TO THE EDITOR

Transiting exoplanets from the CoRoT space mission

V. CoRoT-Exo-4b: Stellar and planetary parameters [★]

Moutou, C.¹, Bruntt, H.², Guillot, T.³, Shporer, A.⁴, Guenther, E.⁵, Aigrain, S.⁶, Almenara, J.M.⁷, Alonso, R.¹, Auvergne, M.⁸, Baglin, A.⁸, Barbieri, M.¹, Barge, P.¹, Benz, W.⁹, Bordé, P.¹⁰, Bouchy, F.¹¹, Deeg, H.J.⁷, De la Reza, R.¹², Deleuil, M.¹, Dvorak, R.¹³, Erikson, A.¹⁴, Fridlund, M.¹⁵, Gillon, M.¹⁶, Gondoin, P.¹⁵, Hatzes, A.⁵, Hébrard, G.¹¹, Jorda, L.¹, Kabath, P.¹⁴, Lammer, H.¹⁷, Léger, A.¹⁰, Llebaria, A.¹, Loeillet, B.^{1,11}, Magain, P.¹⁸, Mayor, M.¹⁶, Mazeh, T.⁴, Ollivier, M.¹⁰, Pätzold, M.¹⁹, Pepe, F.¹⁶, Pont, F.⁶, Queloz, D.¹⁶, Rabus, M.⁷, Rauer, H.^{14,21}, Rouan, D.⁸, Schneider, J.²⁰, Udry, S.¹⁶, and Wuchterl, G.⁵

(Affiliations can be found after the references)

Received / Accepted

ABSTRACT

Aims. The CoRoT satellite has announced its fourth transiting planet (Aigrain et al. 2008) with space photometry. We describe and analyse complementary observations of this system performed to establish the planetary nature of the transiting body and to estimate the fundamental parameters of the planet and its parent star.

Methods. We have analysed high precision radial-velocity data, ground-based photometry, and high signal-to-noise ratio spectroscopy.

Results. The parent star CoRoT-Exo-4 (2MASS 06484671-0040219) is a late F-type star of mass of 1.16 M_{\odot} and radius of 1.17 R_{\odot} . The planet has a circular orbit with a period of 9.20205d. The planet radius is 1.19 R_{Jup} and the mass is 0.72 M_{Jup} . It is a gas-giant planet with a "normal" internal structure of mainly H and He. CoRoT-Exo-4b has the second longest period of the known transiting planets. It is an important discovery since it occupies an empty area in the mass-period diagram of transiting exoplanets.

Key words. planetary systems – techniques: photometry – techniques: radial velocity – stars: fundamental parameters

1. Introduction

The masses and radii of extrasolar planets are fundamental parameters for constraining the physics at play in their interiors. A combination of photometric and Doppler techniques is presently the only way to indirectly derive these parameters. However, this possibility is limited to planets that transit in front of their stars, hence a sample of objects that is highly biased towards close-in orbits.

The planet search programme conducted from space by CoRoT (Baglin et al. 2006) is currently monitoring tens of thousands of stars and is regularly discovering new transiting planets (Barge et al. 2008; Alonso et al. 2008; Deleuil et al. 2008a). CoRoT has the ability to discover planets with smaller radii and/or longer periods than what is routinely achieved by ground-based transit surveys. The evolution of fundamental parameters of extrasolar planets will thus be explored as a function of the distance to the star and as related characteristics like irradiation. This has important implications for our understanding of these planets. For example, it is a way to test whether tidal damping (highly dependent on orbital distance), increased opacities,

or alternative theories are the explanation for the anomalously large sizes of some extrasolar planets (e.g. Guillot et al. 2006; Burrows et al. 2007; Chabrier & Baraffe 2007).

With the current detection threshold of the first CoRoT run (45 day duration), 26 transiting events were detected. Two of them turned out to be planets (CoRoT-Exo-1b and 4b, Barge et al. (2008); Aigrain et al. (2008), 2 are grazing eclipsing binaries, 7 are low-mass binaries, and 10 are background eclipsing binaries. Four events remain unsolved cases, either because they are fast rotators (no possible radial velocity follow-up, the cross-correlation function is too wide or undetected with HARPS) or because they showed no radial-velocity variations. These cases are still in the list of systems to be observed at the next visibility season with higher accuracy. The statistics achieved on this run is compatible with expectations and the simulations on CoRoT detection, with its current threshold and follow-up performances.

The present paper focuses on the fourth planet discovered by CoRoT. The detection and light curve analysis is described in a companion paper (Aigrain et al. 2008, hereafter Paper IV). With its 9.20205d period, the planet CoRoT-Exo-4b has the second longest period known so far in the family of transiting planets, after HD 17156b (Barbieri et al. 2007). We conducted a series of complementary observations from the ground to establish the planetary nature of CoRoT-Exo-4b and to derive the fundamental parameters of both the star and the planet.

Send offprint requests to: e-mail: claire.moutou@oamp.fr

[★] Based on observations obtained with CoRoT, a space project operated by the French Space Agency, CNES, with participation of the Science Programme of ESA, ESTEC/RSSD, Austria, Belgium, Brazil, Germany and Spain; and on observations made with the SOPHIE spectrograph at Observatoire de Haute Provence, France (PNP.07B.MOUT), and the HARPS spectrograph at ESO La Silla Observatory (079.C-0127/F).

2. Observations

2.1. Photometric observations

The photometric measurement was performed on-board CoRoT in an aperture that is adapted to each star and is trapeze shaped, with a solid angle close to that of a 14 arcsec diameter circle. It means that a faint eclipsing binary in the vicinity of the main target can produce a transiting event diluted enough to mimic a planetary signal (Brown 2003). The contamination factor of CoRoT-Exo-4 is estimated from the CoRoT entry catalogue EXODAT (Deleuil et al. 2008b) to be extremely low, i.e. only 0.3% of the light comes from neighbouring stars. The first step in establishing the nature of the transiting body is to check the photometric behaviour of the stars in the vicinity of the target, and especially those that fall inside the photometric aperture mask. This is easily done with ground-based telescopes.

CoRoT-Exo-4 was first observed from the Wise Observatory 18-inch telescope (Brosch et al. 2008) on November 12, 2007. Only a partial transit was recorded, thus preventing a precise estimate of the transit depth (of about 1.4%, which should be compared to the out-of-transit scatter of 0.16% in 5-min bins), but it is important that no significant variation was observed in nearby stars. Another transit event was observed with the Euler Camera (120-cm Swiss Telescope at La Silla Observatory) on November 30th, 2007. Two time series of about 40-min were collected in the star field, with a reference series taken at a similar elevation but one night prior to the transit. The transit depth was estimated to be $1.2 \pm 0.15\%$, in agreement with the CoRoT measurements (1.1%). Finally, the ingress of another transit was observed at the Canada-France-Hawaii Telescope with MegaCam on December 10, 2007. Again, only a partial transit was observed, and the transit depth was not fully reliable.

The three sets of photometric follow up confirm that 1) the transit observed by CoRoT occurs on the central target at the predicted epochs, 2) no star encompasses a deep eclipse, or even a short-term variation, in the vicinity of the target, 3) the transit depth is compatible with the depth measured by CoRoT (i.e. no strong dilution by background objects). A detailed analysis of these data will be given in Deeg et al. (in preparation).

2.2. Radial velocity observations

Seven radial velocity measurements of CoRoT-Exo-4 were obtained with SOPHIE on the 1.93m telescope at Observatoire de Haute Provence (France), from October 31, 2007 to February 2, 2008. These first data points established the planetary nature of the companion, showing a detectable and low-amplitude, radial-velocity variation in phase with the CoRoT ephemeris. Thirteen additional measurements were also obtained with HARPS (3.6m telescope at La Silla, ESO, Chile), from November 19, 2007 to January 21, 2008.

Both instruments are cross-dispersed, fiber-fed échelle spectrographs on which precise radial-velocity measurements were performed with regular Th-Ar calibration observations and the reduction involves cross-correlation techniques (Baranne et al. 1996; Pepe et al. 2002). With SOPHIE, the high-efficiency mode was used with a resolving power of 40,000, and the sky background was simultaneously recorded to correct for contamination (Bouchy 2006). The radial velocities were obtained with a weighted cross correlation of the extracted spectra with a numerical mask corresponding to a G2 star.

The data are listed in Table 2 (available in the on-line version) and shown in Fig. 1. The orbital solution was derived us-

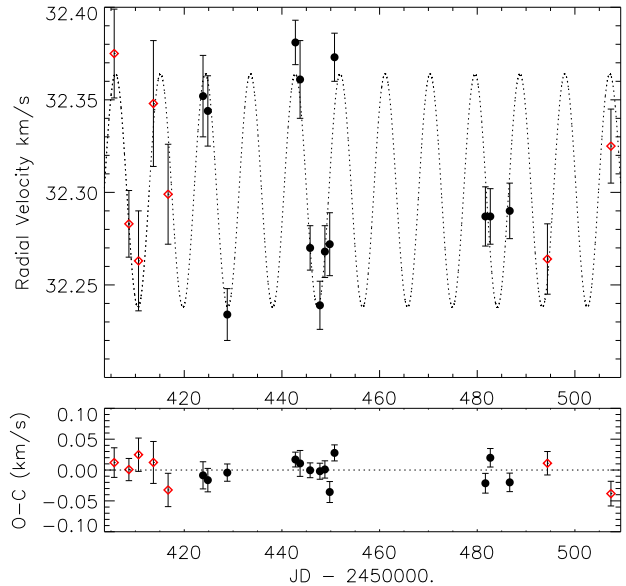


Fig. 1. Radial-velocity measurements of CoRoT-Exo-4 as a function of time, showing the best-fit solution and $O - C$ residuals. Black filled circles are HARPS data, and red open diamonds are SOPHIE data.

ing the combined HARPS and SOPHIE datasets. In the fit we included a constant offset between the two sets of measurements. The ephemeris of the CoRoT light curve was used to constrain the solution. The data were best-fitted with a circular Keplerian orbit of semi-amplitude of 63 ± 6 m/s. When using the 13 HARPS data points alone, the residual rms is 17.6 m/s. With the combined SOPHIE and HARPS datasets (20 measurements), the residual rms is 19.4 m/s. The offset between SOPHIE and HARPS data is only 5 m/s. Figures 1 and 2 show the data and the best fit as a function of time and orbital phase. The $O - C$ time series does not show any variations that would indicate a second massive body in the system with a baseline of 100 days (Fig. 1).

The bisector analysis is shown in Fig. 3. The errors on the span of the bisector slopes are twice as large as for the peak position of the cross-correlation function. The behaviour of the bisector span (BIS) with respect to the radial velocity shows a dispersed relation with little or no trend. Given that short-term variations are seen in the CoRoT light curve (see with Fig. 2 in Paper IV), we tentatively interpret these variations as possibly stemming from a residual of stellar activity.

2.3. Determination of spectroscopic parameters

From radial velocity observations we estimated the projected velocity of the parent star. The result is $v \sin i = 6.4 \pm 1$ km/s, based on the width of the cross-correlation functions from SOPHIE and HARPS. This agrees with a direct comparison of the observed spectrum with a rotationally broadened synthetic spectrum. With our determination of the stellar radius $R_{\star} = 1.15 R_{\odot}$ (see below), this translates into a rotational period of the star ranging between $P_{\text{rot}} = 8.5$ and 10.0 days. This value for the rotation period is compatible with the analysis in Paper IV, and is consistent with a synchronicity of the stellar rotation and the planet orbit.

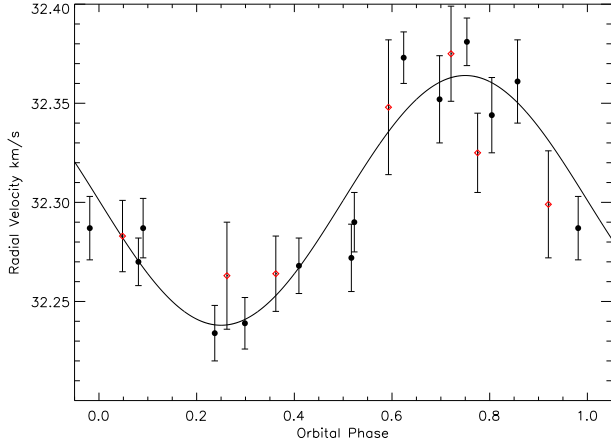


Fig. 2. Radial-velocity measurements of CoRoT-Exo-4 with respect to the orbital phase as estimated from the CoRoT ephemeris and the best-fit solution. Black filled circles are HARPS data, and red open diamonds are SOPHIE data.

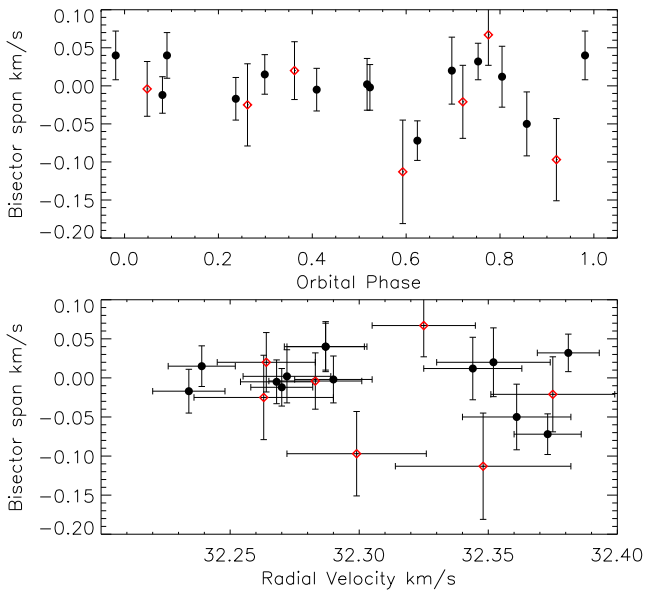


Fig. 3. Bisector variations (span of the bisector slope) as a function of orbital phase (top panel) and radial velocity value (bottom panel). Black filled circles are HARPS data, and red open diamonds are SOPHIE data.

We determined the fundamental parameters of the host star by analysing a HARPS spectrum. The signal-to-noise (S/N) level in the continuum is around 60 per pixel in the range 5 000–6 000 Å and it decreases to 40 in the red and blue parts. The spectrum was carefully normalized by identifying continuum windows in a synthetic spectrum calculated with the parameters of the target star. A spline function was fitted to the continuum windows and divided into the observed spectrum to obtain the normalized spectrum. We made sure that the shapes and depths of lines in adjacent spectral orders were in good agreement. In the final spectrum, the orders were merged and the overlapping parts added using weights based on the measured S/N.

We analysed the normalized spectrum using the semi-automatic software package VWA (Bruntt et al. 2004, 2008). More than 600 mostly non-blended lines were selected for analysis in the wavelength range 3 980–6 830 Å. The VWA uses atmosphere models interpolated in the grid by Heiter et al. (2002) and atomic parameters from the VALD database (Kupka et al. 1999). Abundances were calculated relative to the solar spectrum from Hinkle et al. (2000) following the approach by Bruntt et al. (2008). The VWA automatically adjusts the parameters (T_{eff} , $\log g$, microturbulence) of the applied atmospheric model to get consistent results for all iron lines. The program iteratively minimizes the correlation between the abundance and equivalent width found from weak Fe I lines (equivalent widths < 80 mÅ), the correlation of abundance and excitation potential of Fe I lines (equivalent widths < 140 mÅ), and the mean abundance of neutral and ionized Fe lines must yield the same result. To estimate the uncertainty on the derived parameters and abundances of individual elements, we measured the sensitivity of the results when changing the parameters of the atmospheric model (see Bruntt et al. 2008).

The result is $T_{\text{eff}} = 6190 \pm 60$ K, $\log g = 4.41 \pm 0.05$, and a microturbulence $\xi_r = 0.94 \pm 0.07$ km s⁻¹. The determined spectroscopic parameters do not depend on the adopted value of $v \sin i$. The overall metallicity is found as the mean abundance of the elements with at least 20 lines (Si, Ca, Ti, Cr, Mn, Fe, Ni) yielding $[M/H] = +0.05 \pm 0.07$. Details on individual abundances of CoRoT host stars will be given in a later paper.

3. Estimation of the stellar and planetary parameters

3.1. Stellar mass, radius, and age

Using evolutionary tracks (Siess et al. 2000; Morel & Lebreton 2007), the spectroscopic determination of T_{eff} and the ratio $M_s^{1/3}/R_s$ estimated from the CoRoT photometry (Paper IV), we derived the following estimates for the mass and radius of the star: $M_s = 1.16^{+0.03}_{-0.02} M_{\odot}$ and $R_s = 1.17^{+0.01}_{-0.03} R_{\odot}$. This corresponds to a surface gravity of $\log g = 4.37 \pm 0.02$, which agrees with the spectroscopic value of 4.41 ± 0.05 .

While the details of the process of how lithium is depleted in F-stars is not yet fully understood, it is now well-established that lithium is depleted for stars with a temperature below 6 200 K (Steinhauer & Deliyannis 2004). However, lithium depletion in F-stars is expected to be slow, and data taken for stars with the same age and spectral type show a huge scatter in the equivalent width. By comparing the equivalent width of the Li I line at $\lambda 6708$ (35.2 ± 4.8 mÅ) of CoRoT-Exo-4b with the data for the Hyades (Boesgaard & Tripicco 1986; Thorburn et al. 1993), the UMa moving group (Soderblom et al. 1993), and NGC 3960 (Prisinzano & Randich 2007), an age of about $1^{+1.0}_{-0.3}$ Gyr is the most likely estimate for CoRoT-Exo-4b.

3.2. Planetary mass and radius

Using the values obtained from the transit fit to the CoRoT light curve (Paper IV), the characteristics of the radial-velocity fit, and the stellar parameters from the previous section, we get a planetary mass of $M_p = 0.72 \pm 0.08 M_{\text{Jup}}$ and a planetary radius $R_p = 1.19^{+0.06}_{-0.05} R_{\text{Jup}}$. The semi-major axis of the orbit is $a = 0.090 \pm 0.001$ AU. The mean density of the planet is 0.525 ± 0.15 g cm⁻³. This new planet is found in the expected location of the mass-radius diagram (Fressin et al. 2007). In terms

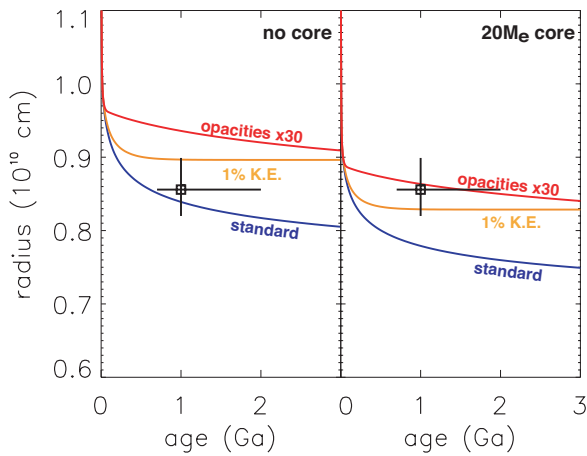


Fig. 4. Theoretical models for the contraction of CoRoT-Exo-4b with time compared to the observations. The models (Guillot et al. 2006) assume either solar composition (left panel) or the presence of a central dense core of $20 M_{\oplus}$ (right panel). In each case, three possible evolution models are shown: (1) a standard model; (2) a model assuming that 1% of the incoming stellar luminosity is transformed into kinetic energy and dissipated in the deep interior by tides, (3) a model in which interior opacities have been arbitrarily increased by a factor 30.

of composition, Fig. 4 shows that it contains a relatively small amount of heavy elements (0 to up to $\sim 30 M_{\oplus}$, depending on the model chosen), as expected from the empirical correlation between stellar metallicity and mass of heavy elements in the planet (Guillot et al. 2006; Burrows et al. 2007; Guillot 2007). The agreement with different models of planetary evolution implies that we cannot rule out any specific scenario used to explain anomalously large planets at this point. However, the discovery of other transiting planets on long-period orbits will be extremely valuable.

4. Discussion

The planet CoRoT-Exo-4b has the second longest period of the transiting systems known today and is found in a region of the mass-period parameter space that was previously empty (see Fig. 5 available on-line).

The mean density of 0.525 g cm^{-3} makes CoRoT-Exo-4b a gas-giant with a “normal” internal structure dominated by H and He. It is located in the bulk of Hot Jupiters in the mass-radius diagram. We estimate the age of the parent star to be about 1 Gyr; thus, the star is likely to be fairly active and its age and rotation rate (Paper IV) are compatible.

New discoveries made with CoRoT will likely populate the mass-period diagram in the period range 5–50 days and allow further investigations of the importance of star-to-planet distance on the internal structure of giant planets. This will complement the output from current radial-velocity surveys, allow us to better understand the mechanisms that govern the contraction of these planets, and provide constraints for planet formation models.

Acknowledgements. We thank the OHP and ESO staff for help provided during the SOPHIE/HARPS observations. The German CoRoT team acknowledges support through DLR grants 50OW0204, 50OW0603 and 50QP0701. HJD and JMA acknowledge support by grants ESP2004-03855-C03-03, and ESP2007-65480-C02-02 of the Spanish Education & Science ministry.

Table 1. The orbit parameters and the fundamental parameters of CoRoT-Exo-4b and its host star.

V_0 [km/s]	32.301 ± 0.005	K [m/s]	63 ± 6
e	0.0 ± 0.1	a [AU]	0.090 ± 0.001
P [d]	9.20205 ± 0.00037		
M_p [M_{Jup}]	0.72 ± 0.08	R_p [R_{Jup}]	$1.190^{+0.06}_{-0.05}$
ρ_p [g/cm^3]	0.525 ± 0.15	T_{eq} [K]	$1,074 \pm 19$
M_s [M_{\odot}]	$1.16^{+0.03}_{-0.02}$	R_s [R_{\odot}]	$1.17^{+0.01}_{-0.03}$
$v \sin i$ [km/s]	6.4 ± 1.0	T_{eff} [K]	6190 ± 60
$\log g$	4.41 ± 0.05	Age [Gy]	$1^{1.0}_{-0.3}$

References

- Aigrain, S., Collier Cameron, A., Ollivier, M., et al. 2008, A&A, submitted
 Alonso, R., Auvergne, M., Baglin, A., et al. 2008, A&A, 482, L21
 Baglin, A., Auvergne, M., Boissard, L., et al. 2006, in COSPAR, Plenary Meeting, Vol. 36, 36th COSPAR Scientific Assembly, 3749
 Baranne, A., Queloz, D., Mayor, M., et al. 1996, A&AS, 119, 373
 Barbieri, M., Alonso, R., Laughlin, G., et al. 2007, A&A, 476, L13
 Barge, P., Baglin, A., Auvergne, M., et al. 2008, A&A, 482, L17
 Boesgaard, A. M. & Tripicco, M. J. 1986, ApJ, 303, 724
 Bouchy, F. 2006, in Tenth Anniversary of 51 Peg-b: Status of and prospects for hot Jupiter studies, ed. L. Arnold, F. Bouchy, & C. Moutou, 319
 Brosh, N., Polishook, D., Shporer, A., et al. 2008, Ap&SS, 314, 163
 Brown, T. M. 2003, ApJ, 593, L125
 Bruntt, H., Bikmaev, I. F., Catala, C., et al. 2004, A&A, 425, 683
 Bruntt, H., De Cat, P., & Aerts, C. 2008, A&A, 478, 487
 Burrows, A., Hubeny, I., Budaj, J., & Hubbard, W. B. 2007, ApJ, 661, 502
 Chabrier, G. & Baraffe, I. 2007, ApJ, 661, L81
 Deleuil, M., Deeg, H., Alonso, R., et al. 2008a, A&A, submitted
 Deleuil, M., Meunier, J.-C., Moutou, C., et al. 2008b, AJ, submitted
 Fressin, F., Guillot, T., Morello, V., & Pont, F. 2007, A&A, 475, 729
 Guillot, T. 2007, ArXiv e-prints, 712
 Guillot, T., Santos, N. C., Pont, F., et al. 2006, A&A, 453, L21
 Heiter, U., Kupka, F., van't Veer-Menneret, C., et al. 2002, A&A, 392, 619
 Hinkle, K., Wallace, L., Valenti, J., & Harmer, D. 2000, Visible and Near Infrared Atlas of the Arcturus Spectrum 3727–9300 Å (ISBN: 1-58381-037-4, 2000.)
 Kupka, F., Piskunov, N., Ryabchikova, T. A., Stempels, H. C., & Weiss, W. W. 1999, A&AS, 138, 119
 Morel, P. & Lebreton, Y. 2007, Ap&SS, 460
 Pepe, F., Mayor, M., Galland, F., et al. 2002, A&A, 388, 632
 Prisinzano, L. & Randich, S. 2007, A&A, 475, 539
 Siess, L., Dufour, E., & Forestini, M. 2000, A&A, 358, 593
 Soderblom, D. R., Fedele, S. B., Jones, B. F., Stauffer, J. R., & Prosser, C. F. 1993, AJ, 106, 1080
 Steinhauer, A. & Deliyannis, C. P. 2004, ApJ, 614, L65
 Thorburn, J. A., Hobbs, L. M., Deliyannis, C. P., & Pinsonneault, M. H. 1993, ApJ, 415, 150

¹ LAM, UMR 6110, CNRS/Univ. de Provence, 38, rue F. Joliot-Curie, 13388 Marseille, France

² School of Physics A28, University of Sydney, Australia

³ OCA, CNRS UMR 6202, BP 4229, 06304 Nice Cedex 4, France

⁴ Wise Observatory, Tel Aviv University, Tel Aviv 69978, Israel

⁵ Thüringer Landessternwarte, 07778 Tautenburg, Germany

⁶ School of Physics, Univ. of Exeter, Exeter EX4 4QL, UK

⁷ Instituto de Astrofísica de Canarias, E-38205 La Laguna, Spain

⁸ LESIA, CNRS UMR 8109, Obs. de Paris, 92195 Meudon, France

⁹ Physikalische Institut Univ. Bern, 3012 Bern, Switzerland

¹⁰ IAS, Université Paris XI, 91405 Orsay, France

¹¹ IAP, CNRS, Univ. Pierre & Marie Curie, Paris, France

¹² Observatório Nacional, Rio de Janeiro, RJ, Brazil

¹³ IfA University of Vienna, 1180 Vienna, Austria

¹⁴ Institute of Planetary Research, DLR, 12489 Berlin, Germany

¹⁵ RSSD, ESA/ESTEC, 2200 Noordwijk, The Netherlands

¹⁶ Obs. de Genève, Univ. de Genève, 1290 Sauverny, Switzerland

¹⁷ IWF, Austrian Academy of Sciences, 8042 Graz, Austria

¹⁸ IAG, Université de Liège, Allée du 6 août 17, Liège 1, Belgium

¹⁹ RIU, Universität zu Köln, 50931 Köln, Germany

²⁰ LUTH, Obs. de Paris, 5 place J. Janssen, 92195 Meudon, France

²¹ ZAA, Technical University Berlin, D-10623 Berlin, Germany

Online Material

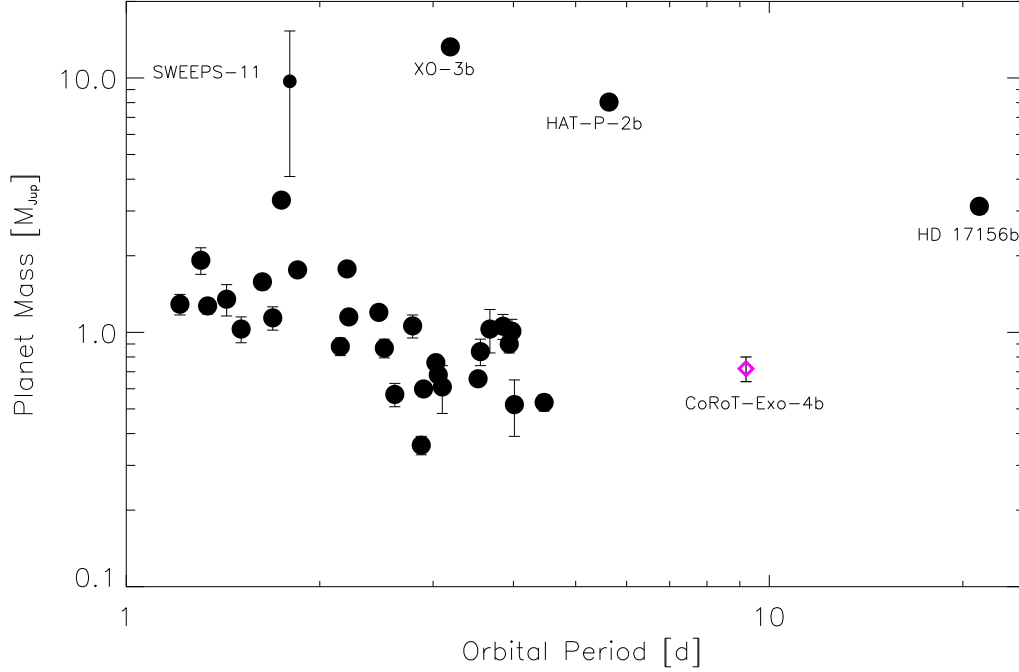


Fig. 5. Mass-period diagram of the 35 known transiting planets showing the location of CoRoT-Exo-4b (diamond).

Table 2. Radial-velocity measurements of CoRoT-Exo-4 with SOPHIE (lines 1 to 7) and with HARPS (lines 8 to 20). "BIS" is the slope of the bisector span, measured in the cross-correlation function.

BJD - 2400000	RV [km s ⁻¹]	Uncertainty [km s ⁻¹]	BIS [km s ⁻¹]	err(BIS) [km s ⁻¹]
54405.6545	32.370	0.024	-0.021	0.048
54408.6667	32.278	0.018	-0.004	0.036
54410.6344	32.258	0.027	-0.025	0.054
54413.6784	32.343	0.034	-0.113	0.068
54416.6908	32.294	0.027	-0.097	0.054
54494.3741	32.259	0.019	+0.020	0.036
54507.3778	32.320	0.020	+0.067	0.040
54423.8430	32.352	0.022	+0.020	0.044
54424.8273	32.344	0.019	+0.012	0.040
54428.8091	32.234	0.014	-0.017	0.028
54442.7618	32.381	0.012	+0.032	0.024
54443.7161	32.361	0.021	-0.050	0.042
54445.7748	32.270	0.012	-0.012	0.024
54447.7813	32.239	0.013	+0.015	0.026
54448.7990	32.268	0.014	-0.005	0.028
54449.7871	32.272	0.017	+0.002	0.034
54450.7729	32.373	0.013	-0.072	0.026
54481.6668	32.287	0.016	+0.040	0.032
54482.6719	32.287	0.015	+0.040	0.030
54486.6509	32.290	0.015	-0.002	0.030